EE3407 Fractal Wifi Antenna

Final Project

Project number: 8. Fractal Wifi Antenna

Name: Miguel Garcia

Last four digits of the 1000x number: 1001070990

Name: Javier Salazar

Last four digits of the 1000x number: 1001144647

Table of Contents

I. OBJECTIVE

The requirements for the fractal antenna are as follows: operate in the 2.4GHz and 5GHz band for wifi application, choose a fractal antenna design, and theoretically verify performance as well as experimental verification to ensure adequate performance. A Sierpinski gasket patch antenna was chosen since it will allow for manufacturing via the pcb mill available in the EE MakerSpace. Moreover, the ease of design makes the antenna more attractive than say a Koch curve which can prove difficult to model in HFSS. Knowing the antenna to be used and the design goals to be met, it's time to dive into the theory which will give a firmer base upon which to begin the design process.

II. THEORY

Patch antennas have pros and cons like any other antenna type. Patch antennas are favorable in industry due to their low profile, inexpensive cost for construction, and easy integration with circuitry design. However, patch antennas have a narrow bandwidth and lower gain when compared to other antennas. Since the antenna is not omnidirectional, then the directivity is higher, typically consisting of 5-8 dB instead of a dipole antenna that is around 1dB.

Due to the nature of the antenna, the triangle iterations determine the resonant frequencies that the antenna will accept best. As a result, the narrowband nature of the antenna will mean a small bandwidth. However, according to Abd Shukur, it has been discovered that the narrow-band property can be transformed into a wide-band antenna by utilizing a "very high dielectric constant substrate and suitable absorbing materials" [1]. Unfortunately, we are limited to the pcb's supplied in the makerspace which contain only FR-1 substrate material.

The design process used for this Sierpinski gasket antenna is as shown in Figure 1A located in appendix A. It begins by setting constraints based on the material used, the number of iterations, and the resonant frequencies desired. The FR-1 material defines the substrate of our antenna to be a non-conductive phenolic resin which is important since the relative dielectric constant can contribute to the bandwidth of the antenna. Once the substrate constraints were known, design moved to the Sierpinski gasket dimensions.

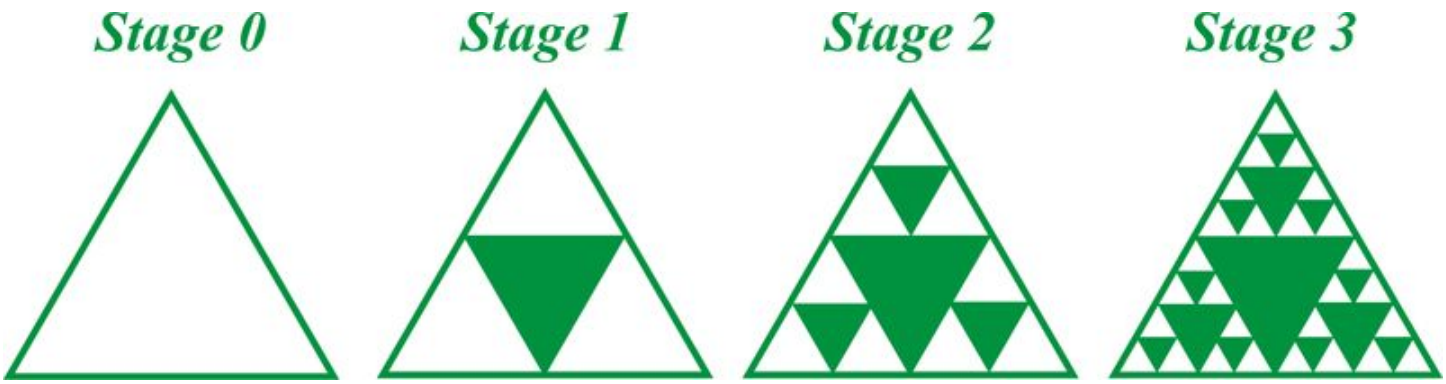

Figure 2. Sierpinski gasket iterations (image courtesy of ck-12.org).

The Sierpinski gasket is a fractal that has an overall shape, usually an equilateral triangle, that subdivides recursively into smaller triangles via iterations [2]. As shown in Figure 2 above, a normal, single triangle is the zero iteration. By cutting a triangle inside, the gasket becomes first iteration. It can be seen that the first iteration contains three small triangles whereas the zero iteration only contains one large triangle. Keeping the pattern going, the fractal evolves to second and third iterations.

An interesting property of the Sierpinski gasket is the ability to capture multiple bands by the iterations of the triangle. Therefore, a first iteration triangle will produce two resonant frequencies. There are applications

where multiple bands are useful such as wifi. Most commercial routers will work in the 2.4GHz and 5GHz range depending on the IEEE 802.11 specifications such as protocol n and ac. Thus, an antenna that can provide maximum power and high bandwidth in this range is the ideal case. The iteration constraints on the gasket set the resonant frequency constraints. The substrate conditions and the frequency conditions are going to determine the size of the iteration triangles.

$$\delta = \frac{h_n}{h_{n+1}} = \frac{f_n}{f_{n+1}}$$

The scale factor of the triangles is given by the equation above where h is the height of the gaskets and f is the frequencies desired. Given that the frequencies needed are 2.4GHz and 5GHz, that will give a scale factor of 2.08 or approximately 2. This means the height of the second largest triangle will be half of the largest triangle as shown in Figure 2 for the first iteration. According to Borja, the simplified frequency equation for the Sierpinski gasket patch antenna is given by the following

$$f_r = k\frac{c}{h}cos(\alpha/2)(\delta)^n$$

where k is a correction constant that equals 0.152 and has a dependent relationship to the substrate type and thickness [4]. The constant k is a good approximation since the FR-1 board is similar to the FR-4 board. c is the speed of light constant in a vacuum and h is the height of gasket for the given frequency. α is the flare angle of the gasket; it is chosen so that we start with an equilateral triangle but make it a variable for HFSS optimization later on. The scale factor is described by earlier equation and the n value is the band natural number so if the frequency is desired on the first iteration then n=1.

Using these equations, the overall dimensions of the gasket are calculated. The height of the largest triangle (i.e. iteration 0) is 65.8mm and the iteration 1 triangles are 32.9mm. From pythagorean theorem, by inspection $a = \frac{2}{\sqrt{3}}h$ where a is the side length of the triangle and h is the height of the gasket and so the outside triangle is 76mm and the iteration 1 triangles are 38mm. The number of iterations determines the resonant frequencies but it is possible to have the interested frequency in another iteration. For example, the 2.4GHz band can be assigned the first iteration but that means that the zero iteration triangle will have to be bigger to fit the first iteration triangles. An advantage of this design is the possibility to shift the iteration return loss curve so that a different bandwidth or return loss coefficient is achieved. However, benefits typically begin to diminish with higher iterations [8]. On another note, it is imperative to leave space between the edge of the substrate and the edge of the antenna since fringing fields will change the directivity of the patch antenna. Now that theory has been discussed, the next step in the design process is to model the Sierpinski gasket in HFSS.

III. Design

A. Antenna Design

It is important to define variables before starting so that the antenna parameters can be optimized after the first initialization. After starting the project, a solution type has to be defined. For the patch antenna, driven modal was chosen as opposed to terminal because modal expresses solutions in terms of incident and reflected powers of waveguide modes of passive, high frequency structures such as patch antennas[3]. Because the feedline is a microstrip (due to patch antenna nature), modal fits the scope of the project. Once selected, a box was made that defines the boundary of the substrate. Given the maximum size the PCB mill can produce, the dimensions are entered as subX, subY, and subZ, where the numbers are 101.6 mm, 127mm, 1.9 mm. The material is defined as FR4_epoxy as it is a close approximation to FR-1 material per Dr. Chiao's suggestion. The ground plane is made by using the rectangle tool and using the same dimensions as the substrate, it is placed at the bottom of the pcb. The boundary "finite conductivity" is chosen so as to model the real world antenna as close as possible. By setting the material to copper and defining the layer thickness as 101 micron from specs of FR-1, the theoretical solution will closely model the experimental solution. Using the polygon tool, a large triangle is made with a smaller triangle inside it to create the first iteration Sierpinski gasket. The

parameters defined in the previous paragraph will be the starting point for the dimensions of these triangles and optimization will be used to give better results. Additional variables are added that stretch the triangle from the edge of the substrate. The scaling terms will define the overall size of the gasket as well as define the flare angle of the triangles. A small microstrip is added from the tip of the triangle to the edge of the substrate since this is the feedline where the EM waves come through. This feedline is given an initial parameter of 10 mm as a starting point and will also be changed during optimization. Finally, the two sheets are united so as to form one conductor on the top side of the substrate. The antenna looks like the figure below.

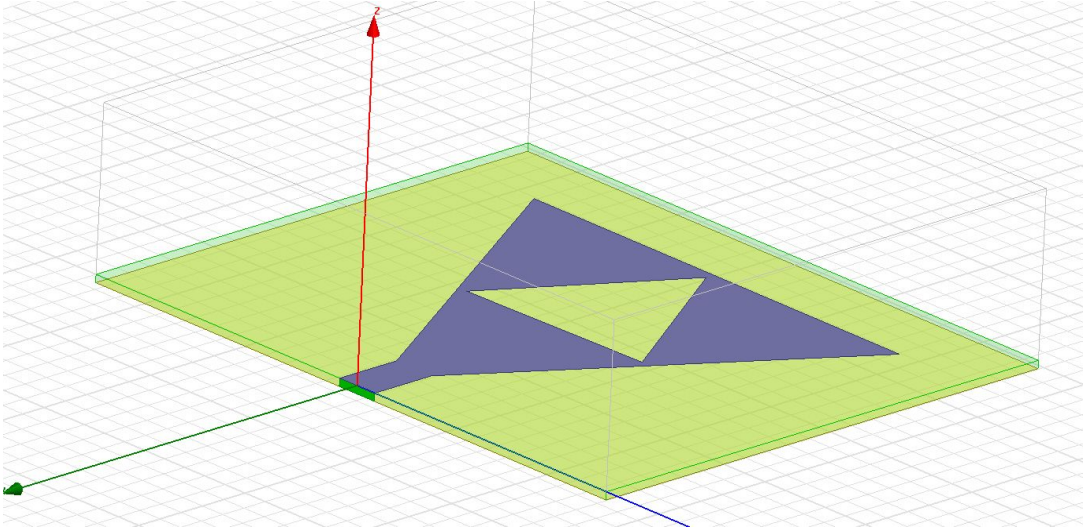

Figure 3. Sierpinski gasket antenna model in HFSS.

Another box is defined on top of the substrate that is extruded 31.25 mm with the material set to air. This is the radiation box that is used for far field information such as gain. A longer radiation box can be used but this will result in more computation time for HFSS solutions. A quarter wave length is the minimum distance required in order to accurately display results because there are no reflected waves and the radiation boundary absorbs all of the radiation [5]. Per HFSS manual, the QW value is based on the solution frequency of the project [7]. Since 2.4 GHz is the interested resonant frequency and the speed of propagation equals the frequency times the wavelength, the result is 31.25 mm. This is based on a wave traveling through air. By selecting the five faces that cover the substrate, a radiation boundary is created as shown in the figure below.

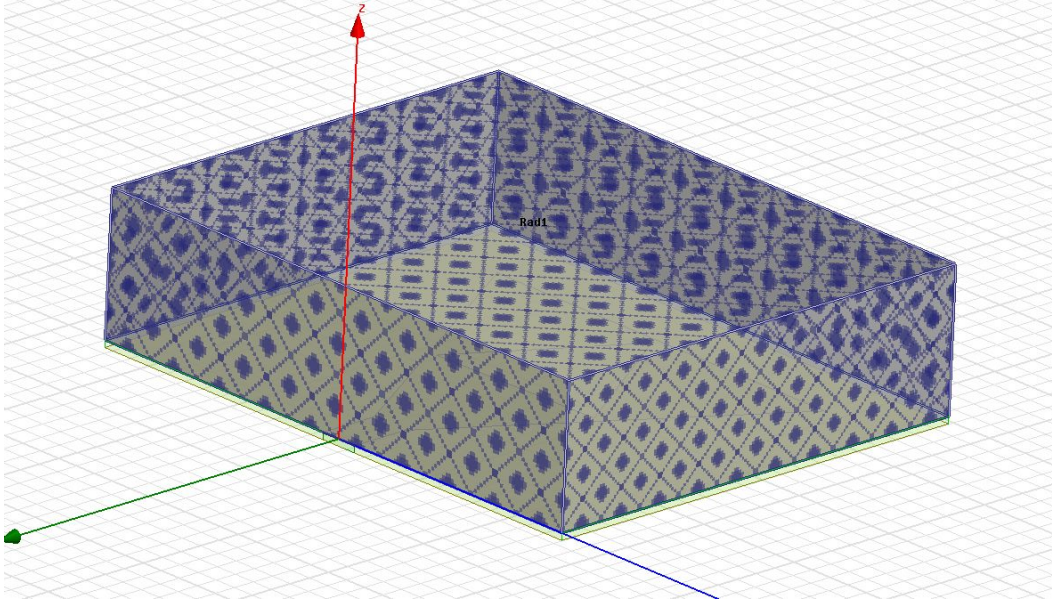

Figure 4. Radiation boundary of patch antenna.

However, to complete the far field set up, an infinite sphere must surround the radiating object so that measurements are recorded for different theta and phi values. A solution set up is added with the following information: solution frequency 2.45 GHz, max. number of passes 30, and max. delta S 0.02. A sweep is added to the setup with a frequency range of 2.2 GHz to 5.5 Ghz and a step size of 0.05 Ghz for the final results. During testing and optimization, this value is limited to only 2.4-2.5 GHz to speed up computations. Finally, an excitation has to be defined before running simulations.

A rectangle is made perpendicular to the ground plane and the Sierpinski antenna on the side of the substrate where the feed line exists. The rectangle is the source which the incoming waves will go through. Appendix C contains a discussion on modeling a coaxial feed system in HFSS. After creating the rectangle, the wave port excitation is used. The integration line is defined as the top of the substrate (antenna) to the bottom of the substrate (ground plane) so that the electric field propagation path is defined to avoid any issues. In theory, the size of the wave port should be as large as the boundary [6]. Therefore, the source rectangle is defined by the feedline parameters. Wave port and lumped port are the two most popular ports used in HFSS. A wave port is on the external boundary only while a lumped port can be internal as well as an external port. However, wave port is useful for exciting stripline, coaxial, and waveguide transmission lines in a more extensive manner than lumped ports because lumped ports are better suited for source structures that are not good transmission lines [7]. Given these reasons, a wave port is chosen and the port impedance is given as 50 Ohms since that is the recognized standard as well as the default option when utilizing the network analyzer. The figure below illustrates the port on the patch antenna.

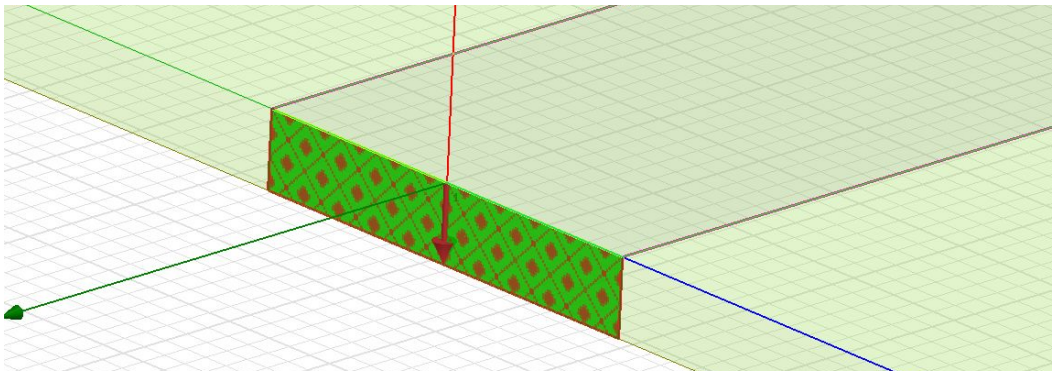

Figure 5. Wave port with integration line visible.

Once these steps are done, a validation check is run to confirm that there are no errors with the project file which is then analyzed and a rectangular plot is generated. However, this is not the final result because these values are the unoptimized values. In the design properties, we check off which values we wish to run during optimization along with the minimum and max values. For the project, the overall gasket scale factor, the feed line width, the flare angle parameter, and the smaller negative triangle scale factor are made optimization parameters. For the setup calculation, VSWR is chosen as the cost function with the goal being to minimize the value. An acceptable cost can be set and once this value is achieved, then the analyzation will stop. However, the default value is left at 0 so that optimization can find the best value possible. In the variables tab, a minimum and maximum step size is selected for the variables in such a way that the max size is large enough to create big steps in the variable range and the minimum step size is small enough to zero in on the correct value. After analyzation, a table in the optimetrics section is generated with different VSWR values based on the input parameter values. It is important to remember that this antenna will be milled so parameters must be chosen so that the spacing between the negative triangle and the large gasket triangle does not become non-existent. In other words, a perfect Sierpinski gasket contains non-manifold vertices but because current has to flow through the bottom triangle to the two upper triangles, there must be spacing to allow current flow. An illustration of this concept is shown below.

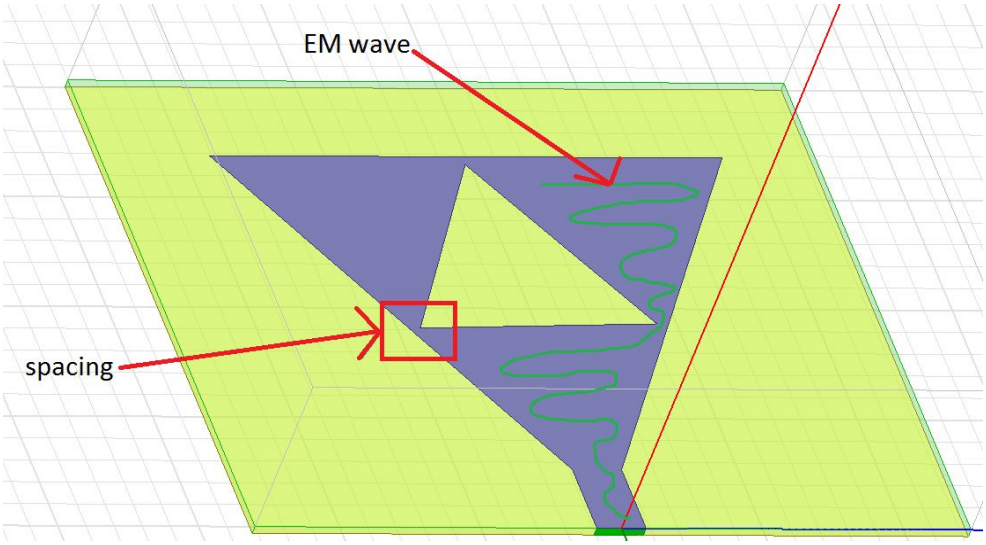

Figure 6. EM waves can only travel if there are no non-manifold vertices.

Once optimization is complete, the parameters are updated and analyzation is run once more without optimetrics and the normal frequency sweep from 2.2 GHz to 5.5 GHz with a 0.05 GHz step size so that smooth and accurate results can be collected. Various plots are collected over the VSWR, the S11 parameter, the far field gain, the far field directivity, and the field radiation pattern.

B. Build Design

The next step in the design process uses Fusion 360 to model the patch antenna before sending it to the mill. Fusion 360 is chosen as the modeling program instead of Eagle per Todd Kelley's suggestion (EE lab technician). Eagle is designed more for schematic based design while Fusion 360 can create custom shapes that can be cut using a mill. Even though HFSS can export dxf files, Fusion 360 imports dxf files as a sculpted object which is the incorrect format needed to generate the proper gcode. Discussing these issues with Todd, Souvik, and further researching the issue online did not result in any solutions. Thus, the antenna had to be completely redesigned within Fusion 360 in order to generate the correct gcode files for the pcb mill.

As stated previously, the .dxf files from hfss can be imported in the Fusion360. These files will appear then as a 2-D sculpted image in Fusion360. This is important because the process by which the gcode files used by the PCB mill are generated through a function called face under the Cam tab. This function takes a series of shapes as inputs and then, based on an input, decides the bit used during milling. The issue found is that the dxf files would not kindly generate a fully scraped mill file but rather only trace the outline of the shapes. To counteract this, the hfss designs were still imported to Fusion360 and once there then they were analyzed. The length of the lines were measured as well as the angles of the triangle shaped. From these measurements, a replica was drawn in Fusion360 using the Model tab.

The issues faced with this process were twofold. The first was in the way the face function was designed. It would draw a line to the edge of the shape and then would commit an about face to begin the next line to be milled. This about face would however eat into the shape of the antenna and so the edges would become a tad bit bumpy instead of the straight edges which were designed. To counteract this, a second function within the Cam tab called trace was used instead. This function is designed to generate a toolpath to trace out the shape designed and in doing so would ensure a straight edge to the triangles. In order to ensure this, a larger bit was used, ⅛" flat tip, for the tracing than the bit used, 1/32" flat tip, for the face function. The second issue, which was only aggravated by the solution to the first, was that the exact center of the bit would follow the line in the gcode which went right around the designed triangles. This was an issue not only in that the milled triangles were often bigger than the designed triangles but they would often eat into the thin bit of copper which allowed current to flow across the antenna. This lead to a rethinking of how the new drawings were done. The

focus was shifted on the angles of the triangles rather than the exact length of their edges which were shortened. These shortened edges were designed from mathematical equations to pull the edges of the triangles inward by $^{1}/_{16}$" so that triangles would maintain their true dimensions on the pcb. Once the design was done, the shapes that were cut out were extruded some distance, 2 mm, so as to give the face and trace functions some depth. These designed toolpaths were then exported as gcode which could be used with by the pcb mill. This gcode was then used on double-sided FR-1 pcb blanks to design the antenna on side with the opposite side serving as a ground plane. To make connections easy a dremel was used to drill a small hole through the feedline through which the inner wire of the BNC cable would be fed and soldered to the antenna while the outer wire remained below and was soldered to the ground plane.

IV. RESULTS

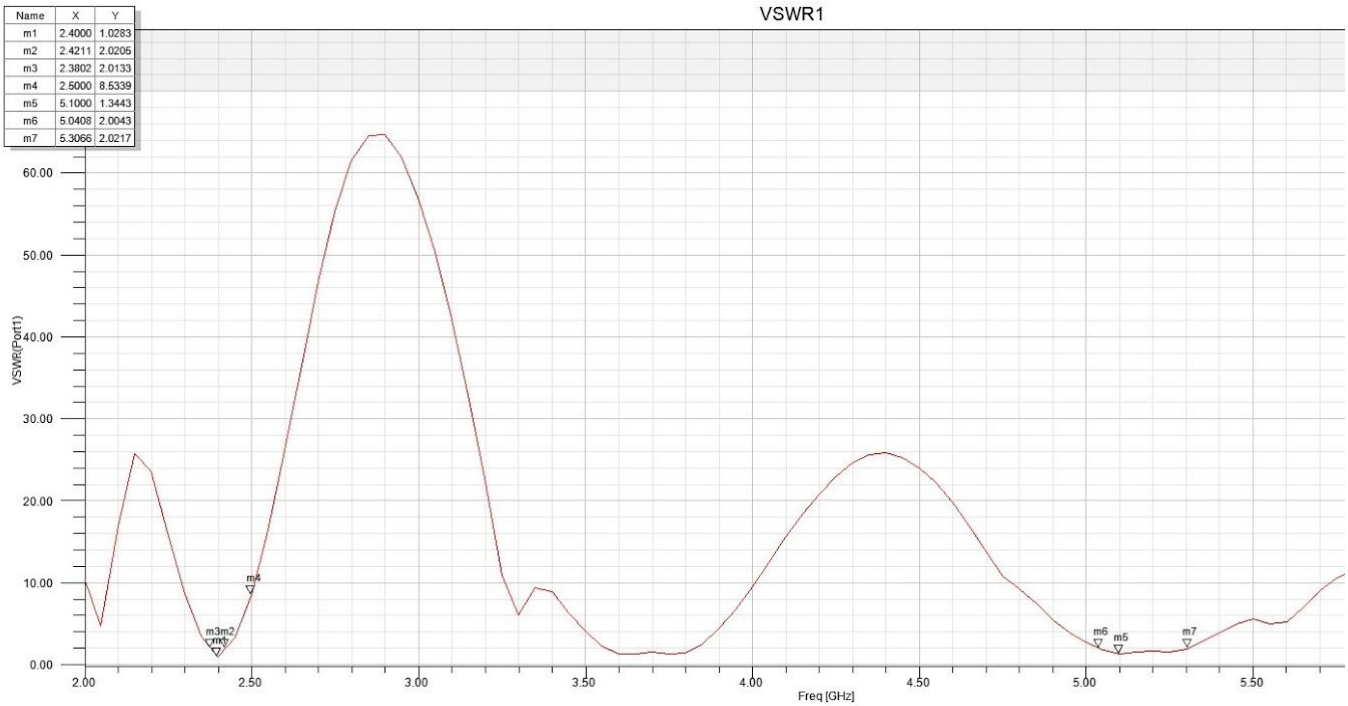

Figure 7. Voltage standing wave ratio.

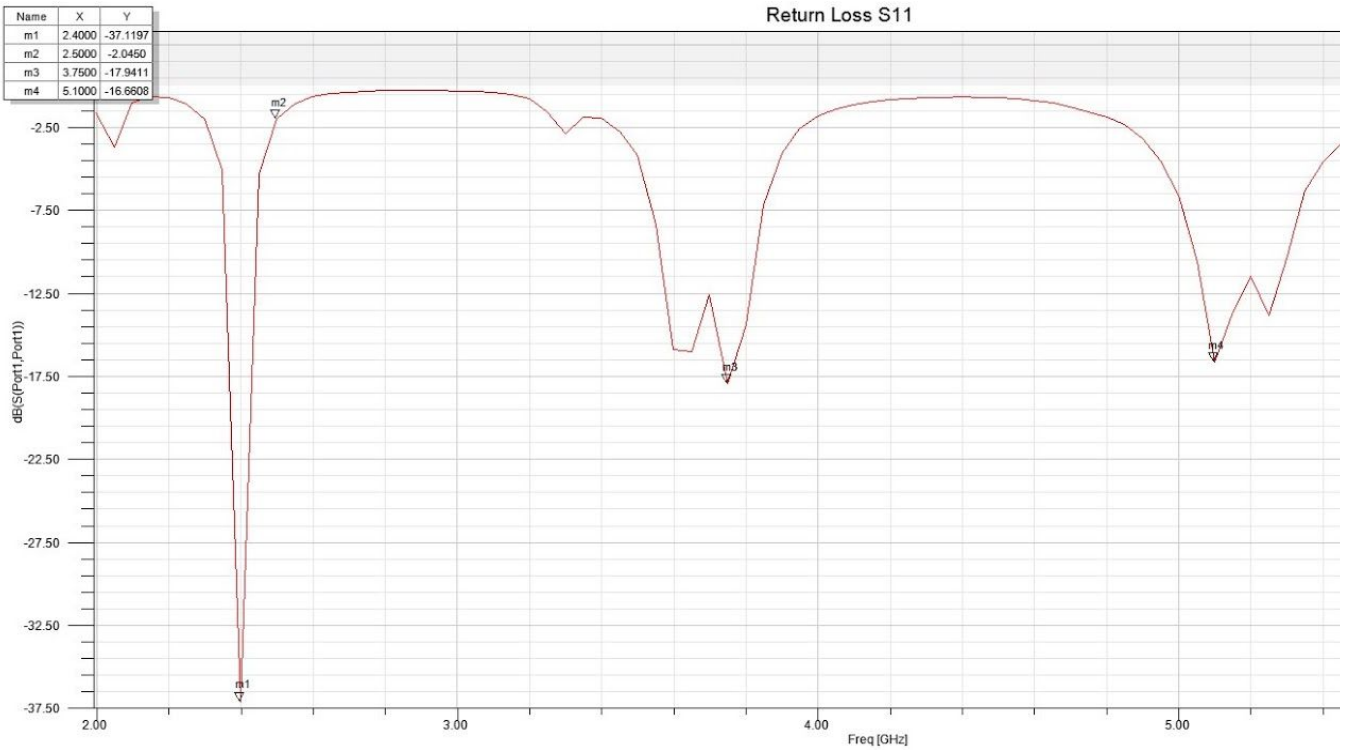

Figure 8. Return loss S11.

Name	Theta	Ang	Mag
m1	0.0000	0.0000	0.9427
m2	180.0000	180.0000	-19.7285
m3	-145.0000	-145.0000	-28.8254
m4	-90.0000	-90.0000	-14.6285
m5	-60.0000	-60.0000	-8.0891
m6	-30.0000	-30.0000	-1.6184
m7	39.0000	39.0000	-3.1382
m8	-38.0000	-38.0000	-3.0700

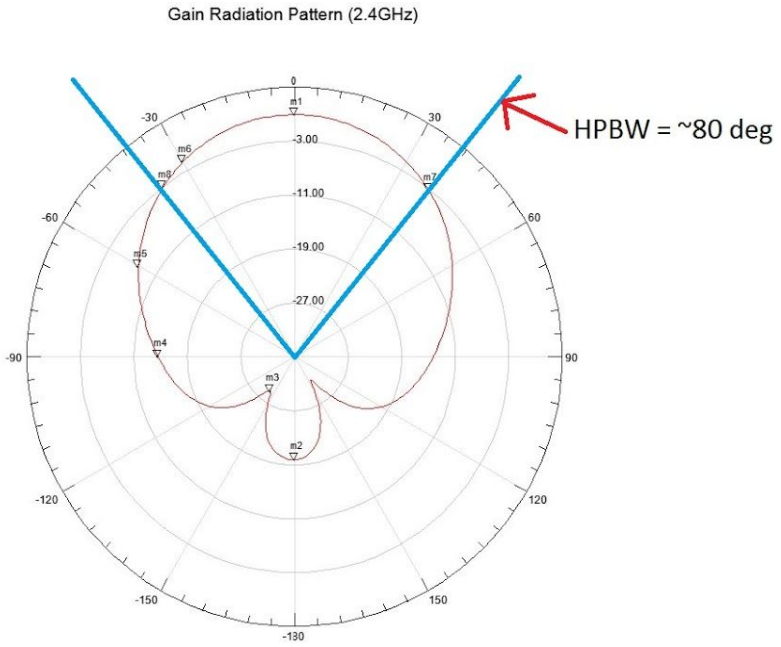

Figure 9. Gain radiation pattern polar plot (phi = 90 deg).

Name	Theta	Ang	Mag
m1	0.0000	0.0000	0.9427
m2	-37.0000	-37.0000	-2.9996
m3	43.0000	43.0000	-2.9107
m4	179.0000	179.0000	-19.5773
m5	-160.0000	-160.0000	-22.4023
m6	90.0000	90.0000	-11.6546
m7	-90.0000	-90.0000	-13.4808

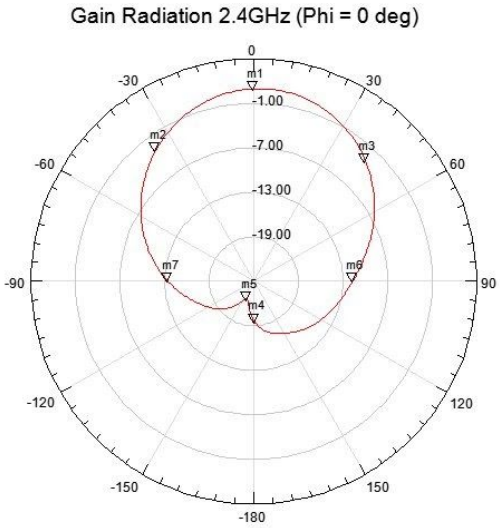

Figure 10. Gain radiation polar plot (phi = 0 deg).

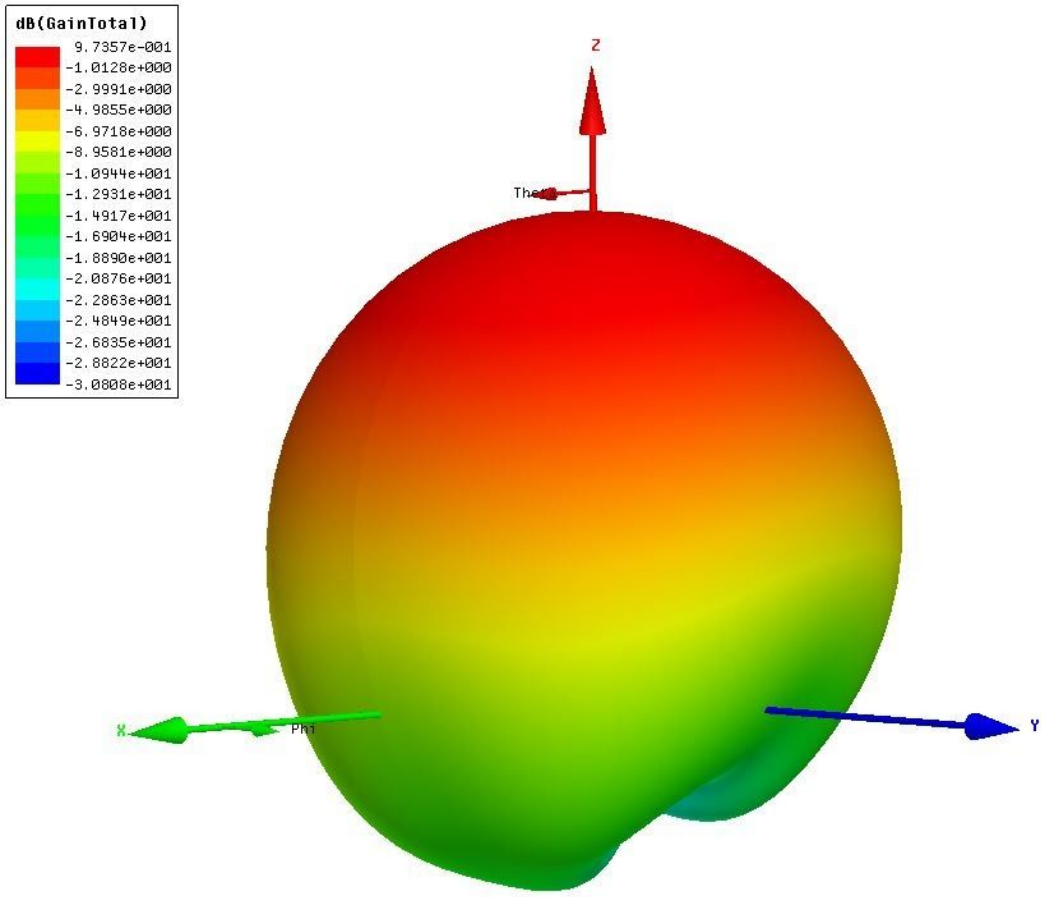

Figure 11. Gain 3D polar front plot.

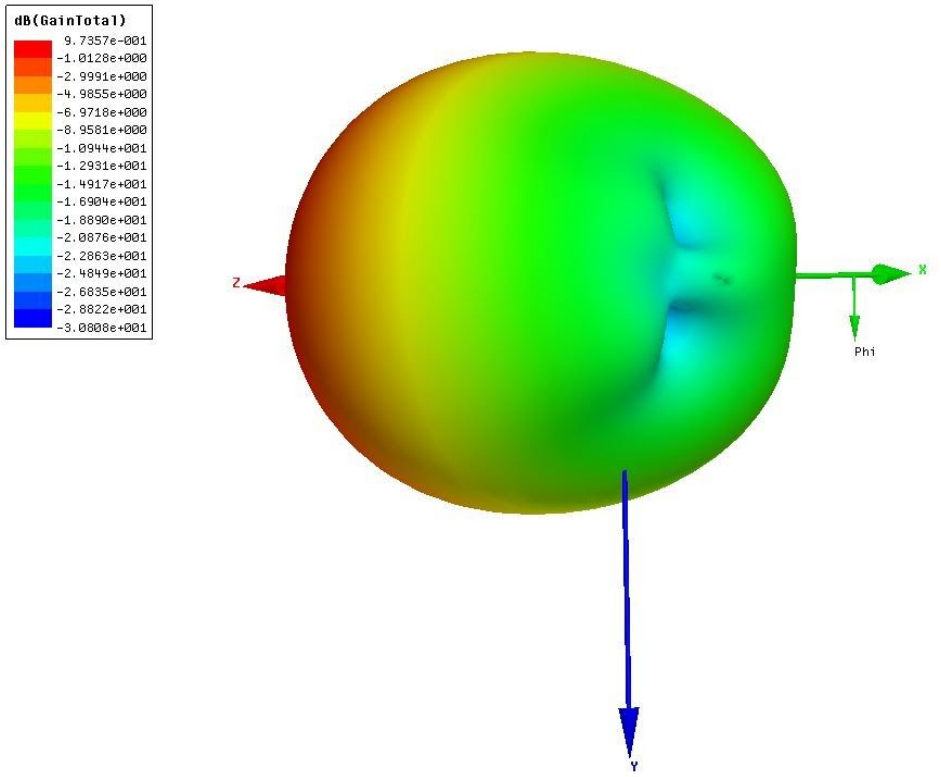

Figure 12. Gain 3D polar back plot .

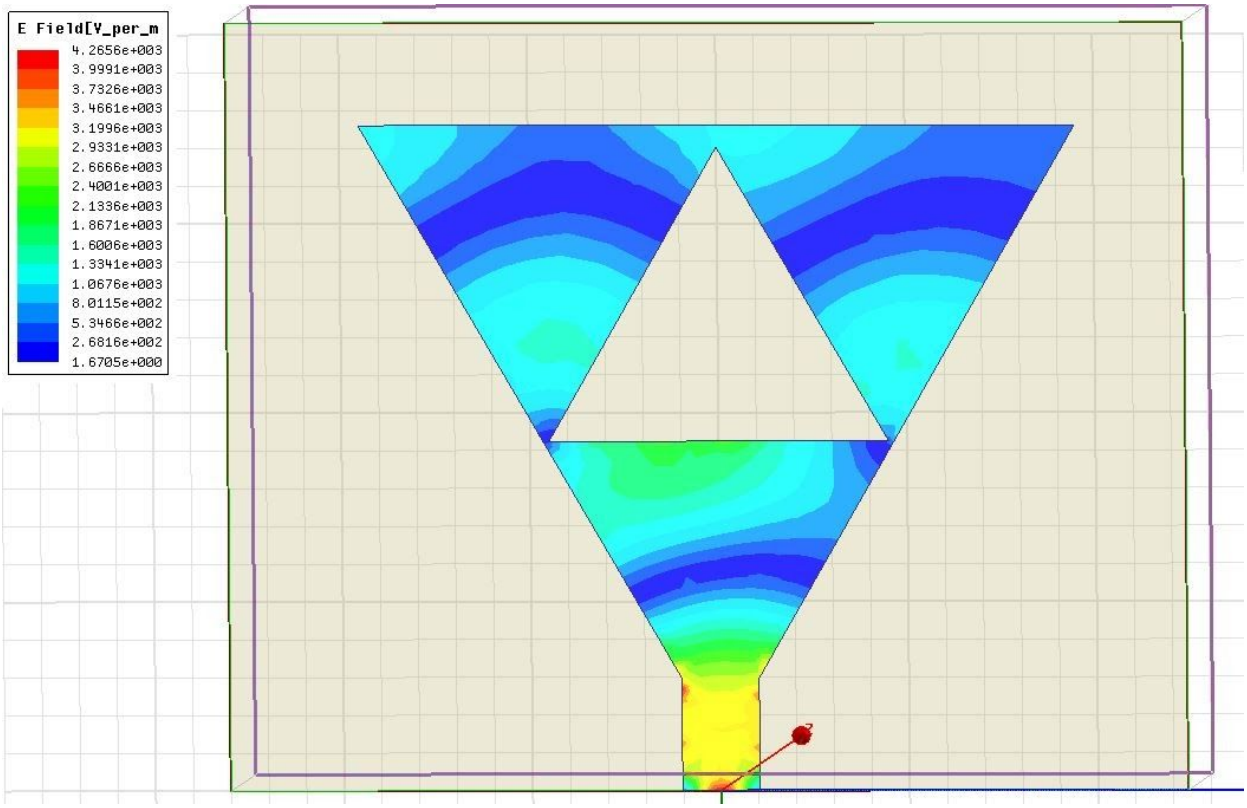

Figure 13. Electric field distribution for 2.4GHz at 90 deg phase.

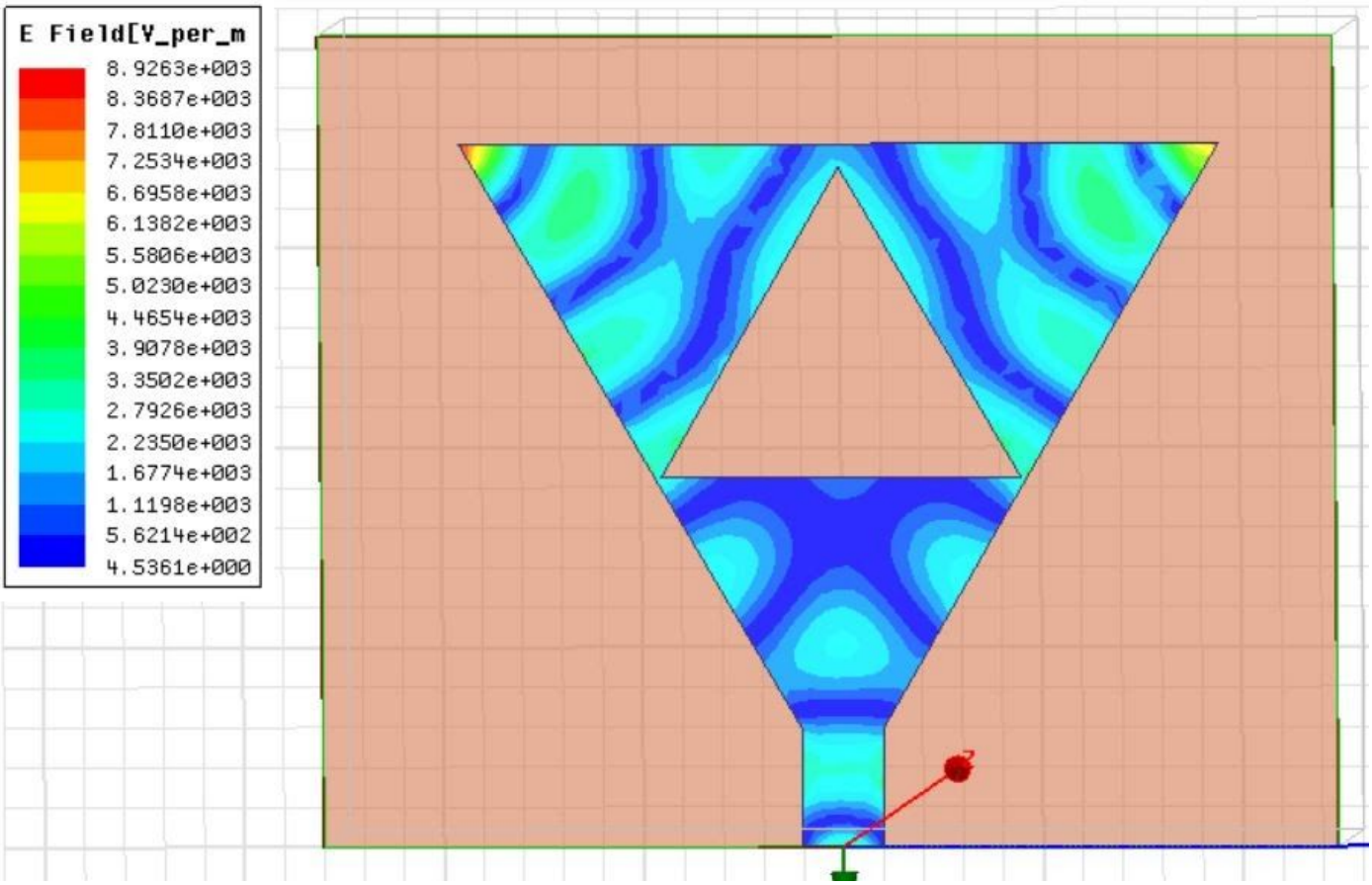

Figure 14. Electric field distribution for 5GHz at 90 deg phase.

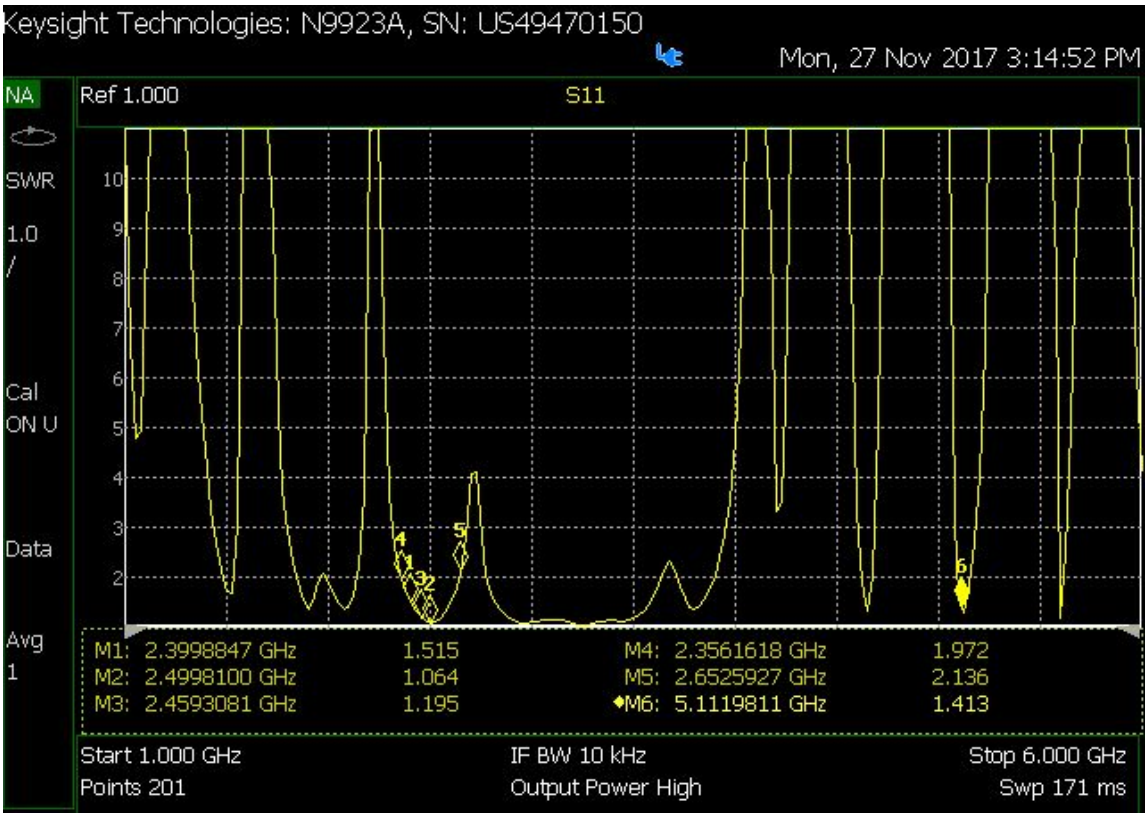

Figure 15. Voltage standing wave ratio VNA data.

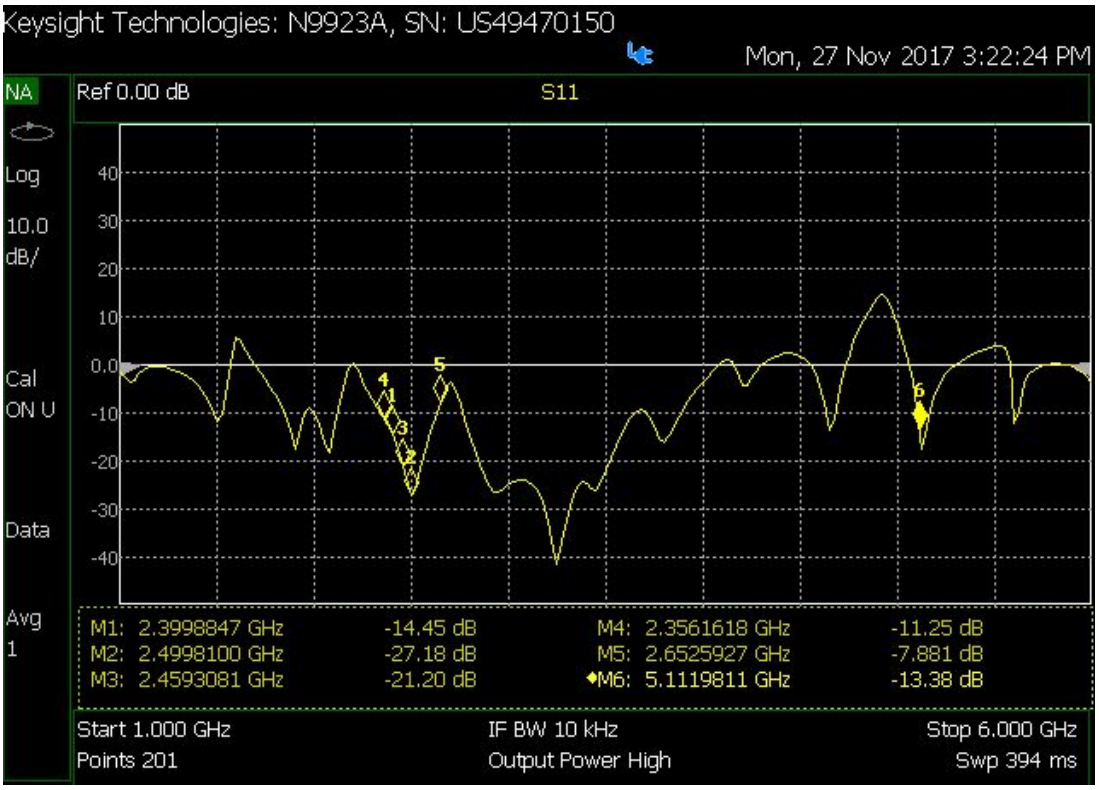

Figure 16. Return loss (dB) VNA data.

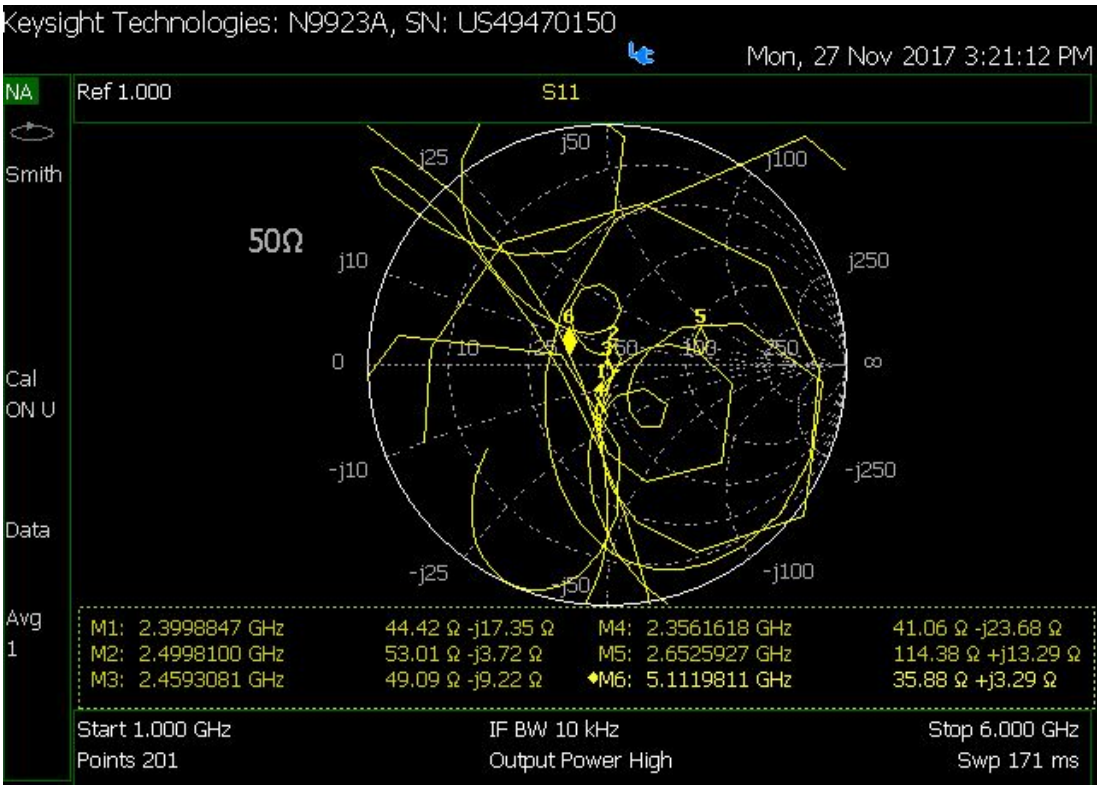

Figure 17. Smith chart (1-6GHz sweep) VNA data.

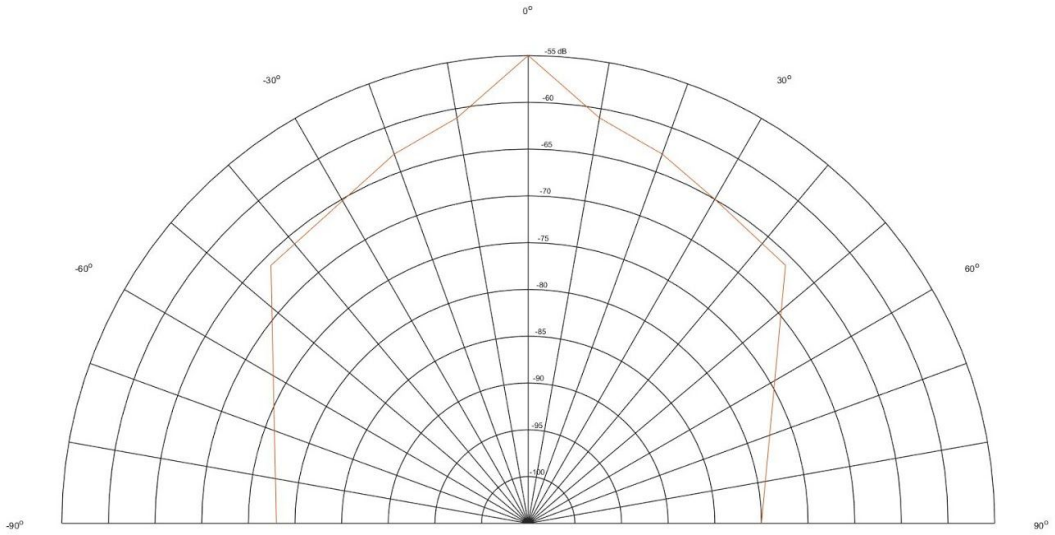

Figure 18. Far field gain (theta sweep -90 to 90 deg) VNA data at phi = 90 deg.

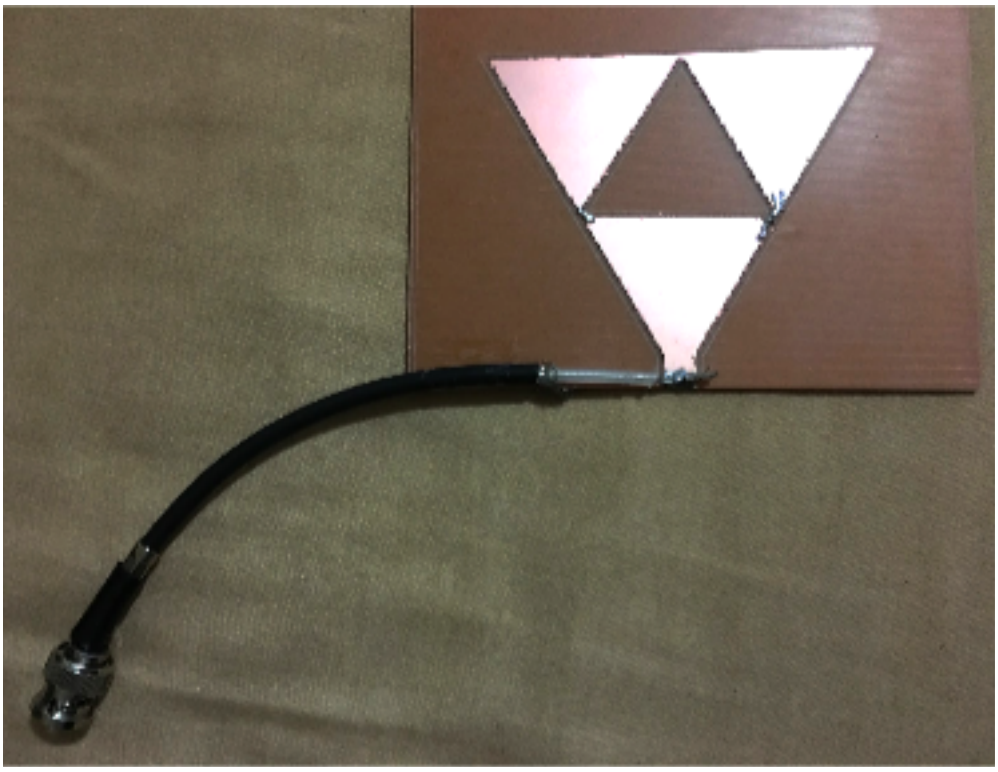

Figure 19. Sierpinski gasket on FR1 PCB.

TABLE 1

Antenna Results			
Data Type	HFSS	VNA	Percent Error
Peak Gain	1dB	NA	NA
Front/Back Ratio	21.4 dB	NA	NA
Radiation Efficiency	31%	NA	NA
BW (2:1 VSWR) 2.4GHz	2%	11.9%	495%
BW (2:1 VSWR) 5GHZ	5.2%	1.3%	75%
-3dB Delta Angle	~80 deg	~100 deg	25%
2.4GHz VSWR	1.03	1.06	2.9%
5GHz VSWR	1.34	1.41	5.2%

V. Discussion

Looking at Figure 7, a 1.03 VSWR is achieved at 2.4GHz while having a 1.34 VSWR at 5.1GHz from HFSS. Careful examination shows another resonant frequency at the 3.5-4 GHz range that appears unexplained. Analyzing the equations for the Sierpinski gasket do not reveal why this frequency works so well. However, running HFSS in this frequency range with an electric field plot reveals the answer. From Figure 20, the electric field plot reveals where the mysterious 3.5GHz signals are being picked up. The feedline is the component responsible for this additional resonant frequency since it is behaving as a small rectangular patch antenna. Since the feedline is incorporated into the HFSS solutions, the resonant frequency at the 3.5GHz range can be disregarded as it does not affect the results.

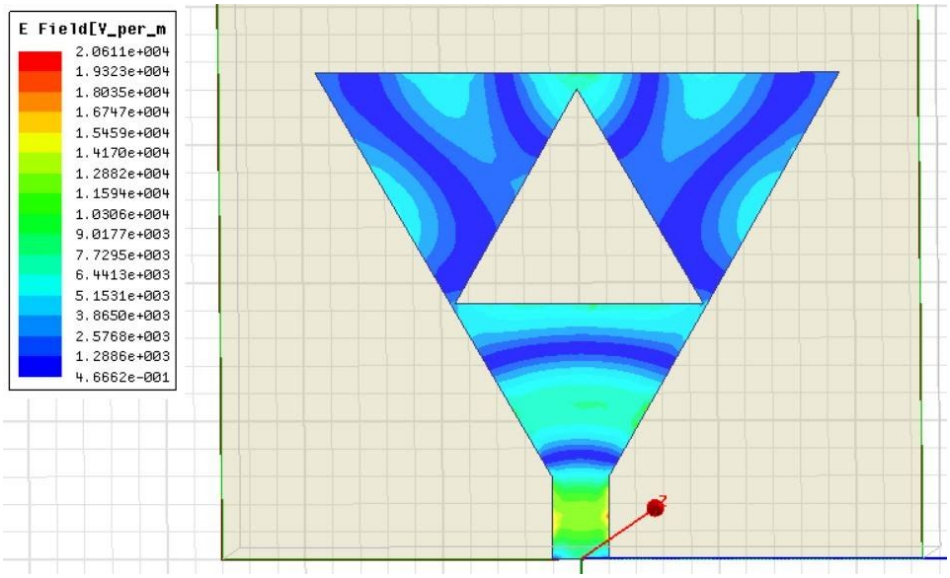

Figure 20. Electric field pattern at 3.5GHz.

Figure 8 shows a very narrow peak that goes to -37dB at 2.4GHz for the return loss. This means that the bandwidth is limited for this range even though the VNA results will prove differently. The HFSS return loss for 5.1GHz is only -16dB indicating that the main antenna function remains at 2.4GHz. Figure 9 and 10 both show the radiation pattern for the antenna. Figure 9 holds phi equal to 90 degrees and performs a sweep around theta. The antenna has a very small back lobe and generally a wide main lobe that has a half power bandwidth of approximately 80 degrees. Figure 10 shows the same information except with phi equal to 0 degrees. Due to the asymmetrical properties of the antenna, Figure 10 is different than Figure 9. If the antenna is reflective across the origin, then symmetry dictates that both figures would be the same. Figures 11 and 12 illustrate the HFSS far field gain information of the antenna for the front and back portions respectively. From the graph, the most intense section reads off a value of 0.97dB which indicates that the max gain is 0.97dB. Typical patch antennas have a gain of 5dB so the antenna simulation value is far from the expected result. It is not known why there is a big discrepancy between simulated result and expected result. However, antenna gain can be improved by implementing an array of patch antennas. A normal gain value for array patch antennas is around 15dB so this is one technique to solve the issue. Figure 13 and 14 show the electric field distribution for 2.4 and 5 GHz respectively. Most of the electric fields appear to be frozen in the feedline section for 2.4GHz. Understanding Sierpinski theory, the 2.4GHz waves should be located all over the zero iteration triangle since the biggest triangle captures those fields. However, HFSS simulations produced a different result than expected. The 5GHz field distribution gave good results where it is apparent that the individual first iteration triangles are traping the 5GHz waves. For both field distrubations, the electric field does not follow a typical distribution curve.

The electric field magnitude is not high at the edge of the patch location opposite to the feedline. This is the ideal distribution and the Sierpinski antenna fails to model the ideal distribution. Appendix B includes a discussion on various attempts to shift the magnitude of the field lines to the edge of the patch antenna. Now that HFSS results have been discussed, the VNA results are discussed below.

Figure 15 displays the voltage standing wave ratio information from the vector network analyzer. Comparing to HFSS simulations, the results are better than expected. A 1.06 VSWR is achieved at 2.4 GHz when a 1.03 VSWR was expected. The curve around 2.4-2.5GHz is much wider than the results gathered from Figure 7. The 3 GHz resonant frequency also shows up here with a very wide bandwidth as can be seen from the figure. From Figure 7 and 15, the bandwidth for 5GHz varies greatly. The HFSS simulations indicate a wide bandwidth while VNA results are narrow. From Figure 17, the smith chart shows that the 2.4-2.5 GHz range contains more capacitive reactance than inductive reactance. Moreover, the resistance is more or less around the 50 Ohm mark. To bring the frequencies closer to the matching point, the flare angle of the triangles can be manipulated so that the capacitance between the triangles can be less thus reducing the negative reactance for example. Another idea is to change the distance between the ground plane and patch antenna or change the area of the ground plane in order to change the reactance since capacitance is a function of area, distance between plates, and permittivity.

For the resistance, scaling the triangles or the feedline can give a better matched impedance value since the amount of metal and the electric flow path is changed. The VNA far field gain information displayed on Figure 18 is not accurate data though the overall shape is retained from the HFSS simulations. At the main lobe location, the gain value is -55 dB which is incorrect. Because the horn antenna uses a special cable, there is no calibration kit in the lab for the horn antenna. Because it is not possible to calibrate properly, the values are not

correct. However, the shape is more or less retained. The back portion of the theta sweep was not performed as it is not possible to perform the measurement in the small lab room. Any signals sent from the horn antenna would reflect from the walls and cause interference with measurements. Therefore, a front/back ratio is not provided in Table 1 since the back lobe information is unavailable.

Since the values of the plot are incorrect, it is not directly possible to measure the -3dB point. However, an approximation can be made because the power steeply drops off after a certain angle. Using this location to generate a half power bandwidth gives a value of 100 degrees which is 15 degrees off the expected 80 degree value. Figure 19 include pictures of the first iteration Sierpinski antenna manufactured from the pcb mill. Table 1 includes a summary of the results from previous figures and from the discussions above. Additionally, a percent error analysis is done for the results in the table. From the table, it is seen that the radiation efficiency between the directivity and the gain is 31%. The substrate material and thickness can affect the radiation efficiency and it is typical for patch antennas to get around 50% efficiency [9]. Additionally, surface waves, waves that propagate along the interface between two media, cause a lower efficiency. Dr. Oraizi has seen an improvement in radiation efficiency by suppressing surface waves [9]. The surface waves move towards the edges of the antenna substrate where they radiate into space. In order to prevent this, Dr. Oraizi has managed to suppress surface waves by removing portions of the substrate close to the metallic patches [9]. In the same way, the substrate can be modified close to the large zero iteration triangle to suppress surface waves and thus improve radiation efficiency. On another note, the front/back ratio is 21dB where typical values are 25dB so the magnitude of front/back lobes is more or less the expected value. On a final note, the antenna was connected to an old Netgear router via PCB soldering and an iPhone was used to test the signal range from the router. The signal app encountered disconnection issues at 125 feet. The test was done inside Nedderman Hall so the results will not be as good as standing outside due to signal interference inside the building. Moreover, the small dipole originally attached to the router achieved a range of 165 feet before experiencing connection issues. One possible reason to explain the difference is below is to assume that the antenna connection on the board is not matched for the standard 50 Ohms. It is likely that the manufacturer built the antenna specifications for some other impedance value that is different from the Sierpinski antenna since the dipole performed better.

VI. Conclusion

In conclusion, in the process of this project we made use of fractal and antenna theory along with hfss to design a Sierpinski gasket patch antenna that operates in the 2.4GHz and 5GHz wifi bands. Once designed, the antenna was copied into Fusion360 to be printed on the Bantam Tools Desktop PCB Milling Machine available in the EE MakerSpace, NH 131. The printed antenna was tested through the Vector Network Analyzer where it was found to have a 1.06 VSWR in the 2.4GHz band and 1.41 VSWR in the 5GHz band. This, along with the other data shown in Table 1, demonstrates that the built antenna operates well in a commercial setting with the only issue being that there is more directivity to the fractal antenna in comparison to most antennas used in wifi routers which are designed to be omnidirectional. Possible applications of fractal and antenna theory are then discussed which may give better results from a Sierpinski gasket patch antenna. Overall, the project was a fantastic method of having students apply their knowledge from Electromagnetics as well as research beyond the general material taught in class, both of which will be quite helpful on any research and design project that students might get in the future.

VII. REFERENCES

[1] ABD SHUKUR. BIN JA'AFAR , "SIERPINSKI GASKET PATCH AND MONOPOLE FRACTAL ANTENNA," thesis, UNIVERSITI TEKNOLOGI MALAYSIA, BUKIT BERUANG, 2005.

[2] TEDESCHINI LALLI Laura, "SIERPINSKI TRIANGLES IN STONE, ON MEDIEVAL FLOORS IN ROME," *Journal of Applied Mathematics*, vol. IV, pp. 1–10, 2011.

[3] HFSS v10 User's Guide. (2017). 1st ed. [ebook] Pittsburgh: Ansoft. Available at: http://anlage.umd.edu/HFSSv10UserGuide.pdf [Accessed 26 Nov. 2017].

[4] C. Borja, J. Romeu, "Multiband Sierpinski fractal patch antenna", *Antennas and Propagation Society International Symposium 2000. IEEE*, vol. 3, pp. 1708-1711 vol.3, 2000.

[5] Ruchti, G. (2017). *Senior Thesis*. [ebook] University of Maryland. Available at: http://anlage.umd.edu/Greg%20Ruchti%20Senior%20Thesis.pdf [Accessed 26 Nov. 2017].

[6] "Wave Ports and Lumped Terminals." National Taipei University of Technology. [Online]. Available: http://www.cc.ntut.edu.tw/~juiching/Ports.pdf.

[7] M. Kopp, "An Introduction to HFSS: Fundamental Principles, Concepts, and Use." ANSOFT, LLC, 2009. [Online]. Available: http://e-science.ru/sites/default/files/upload_forums_files/8u/HFSSintro.pdf.

[8] Khanna, G. and Sharma, N. (2016). Fractal Antenna Geometries: A Review. *International Journal of Computer Applications*, [online] 153(7), pp.29-32. Available at: http://www.ijecs.in/issue/v3-i9/59%20ijecs.pdf [Accessed 16 Nov. 2017].

[9] Oraizi, H. and Rezaei, B. (2011). Improvement of Antenna Radiation Efficiency by the Suppression of Surface Waves. *Journal of Electromagnetic Analysis and Applications*, [online] 03(03), pp.79-83. Available at: https://pdfs.semanticscholar.org/e4dd/a53b0b137c4a2e0cb8d69ae6afd18294f6aa.pdf [Accessed 26 Nov. 2017].

VIII. APPENDIX A (DESIGN FLOW CHART)

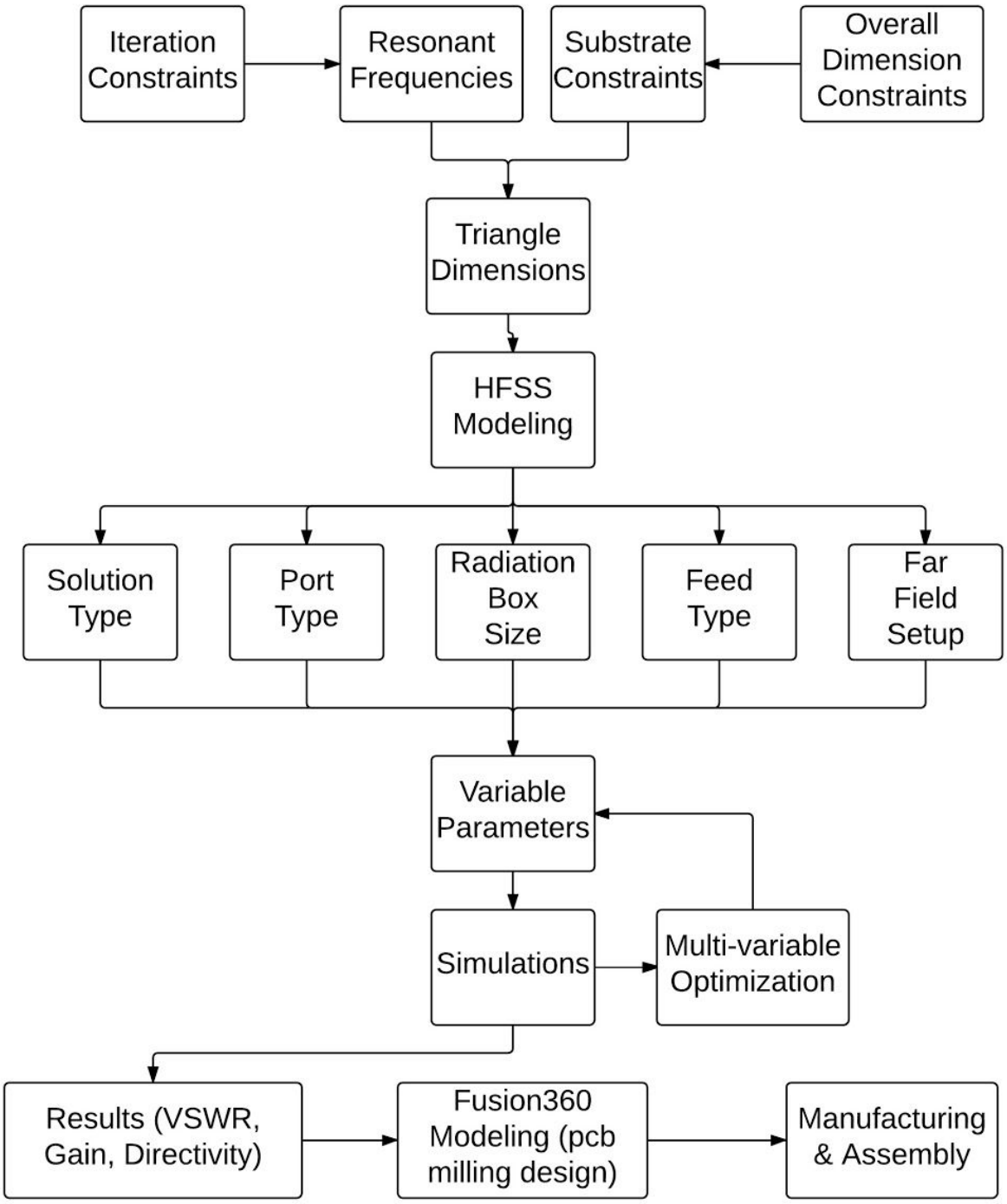

Figure 1A. Fractal antenna design flow chart process.

IX. Appendix B (Electric field redistribution models)

Since the typical electric field distribution of a patch antenna has a big magnitude at the edge located furthest from the substrate, different models were simulated to model this process. Changing the height of the overall triangle, per Dr. Chiao's suggestion, did not redistribute the electric field. One model was simulated with the feedline located on the other end of the substrate as shown in Figure 1B. While there is a larger electric field in this section, the small area is limited to a small location relative to the substrate. In Figure 2B, a thin rectangular bar is cut near the top section of the antenna. The thought process behind this attempt was to reduce the impedance in the top section of the antenna so that the electric fields will shift upwards to an area of lower impedance. While this logic may or may not be true, the results seemed to work okay to bring the electric fields upwards. However, it was not possible to optimize the antenna parameters to give as good of a VSWR. Another attempt resulted in a bowtie Sierpinski triangle which worked worse than the typical Sierpinski triangle. It was not possible to optimize the reflection coefficient for this modification and the electric field ended up weaker than the normal antenna as shown in Figure 3B. Figure 4B shows the effect of squishing the antenna on the electric field distribution. As illustrated, the electric field ended up weaker as well by this result. In summary, none of the results provided significant results and so the regular Sierpinski triangle was used for analysis.

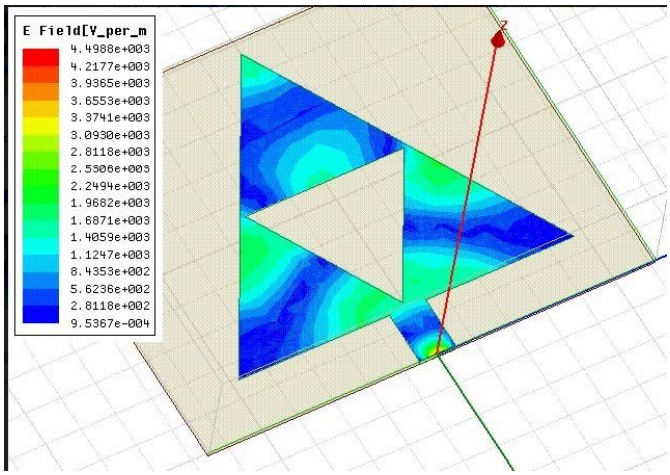

Figure 1B. Flipped feed line antenna.

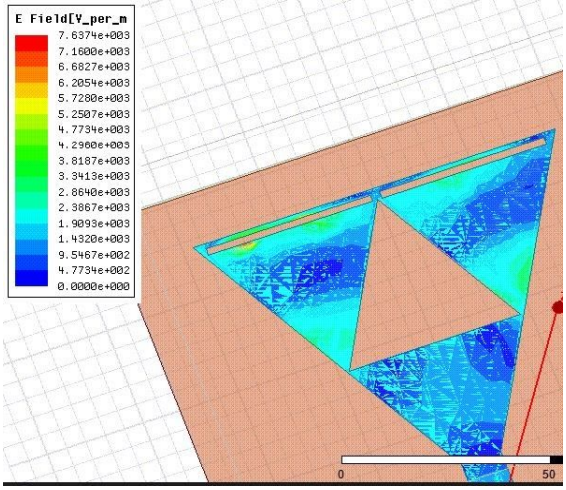

Figure 2B. Antenna with low impedance zone.

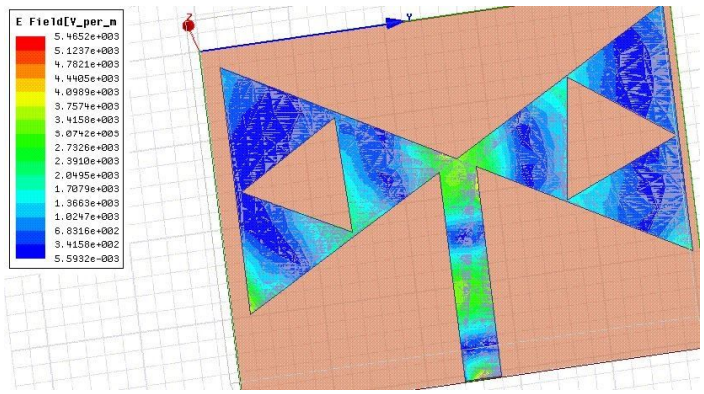

Figure 3B. Bowtie Sierpinski antenna.

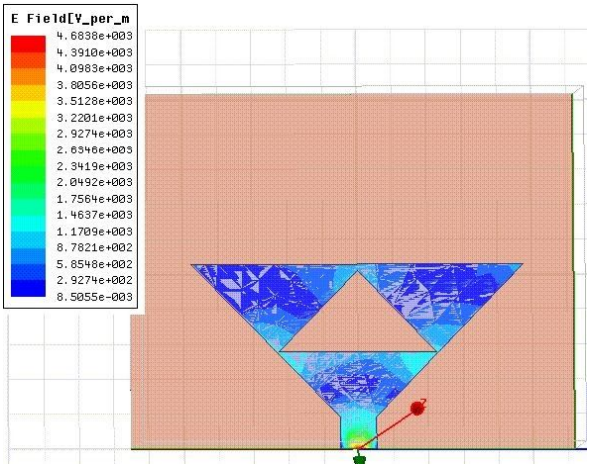

Figure 4B. Shortened Sierpinski antenna.

x. Appendix C (Coaxial feed HFSS modeling)

In HFSS simulations, the wave port is located on the edge of the substrate and this is where the waves are feed. Attempts were made to model the coaxial feed line in HFSS by drawing the inner conductor, insulator, outer conductor, and sleeve jacket according to manufacturer specifications. The cable was set to a reasonable short length that can be achieved in lab. The pin goes from the ground plane to the surface of the patch antenna via the substrate. The outer conductor connects to the ground plane with a PVC insulator in the middle of the two. However, we were unable to get accurate results as the VSWR remained above 15 at all times. Modifications to the design of the coaxial feed did not give accurate results and it is not known why the VSWR remained high. Modeling the antenna via the edge of the substrate yielded accurate results in comparison to VNA results. Therefore, it is safe to say that the effects of coaxial modeling in HFSS can be considered negligible in the calculations of the results. After speaking to Adrian, Adrian said that due to the high frequency nature of Wifi, the length of the transmission cable is negligible since we are using a relatively short transmission line. Because of this discussion and the problems encountered in correctly modeling the HFSS simulation, the coaxial feed was discarded from calculations. Figure 1C shows the coaxial feed in HFSS with the waveport at the edge of the transmission line at the end of the connection. The ground plane is seen connecting to the ground plane and the inner conductor going through the substrate and to the surface of the patch antenna where it connects to the Sierpinski triangle. The ground plane is removed where the cable and the ground plane meet in order to avoid shorting issues between the inner and outer conductors. In conclusion, the wave port on the edge of the substrate was correctly modeled while the coaxial feed could not be modeled correctly.

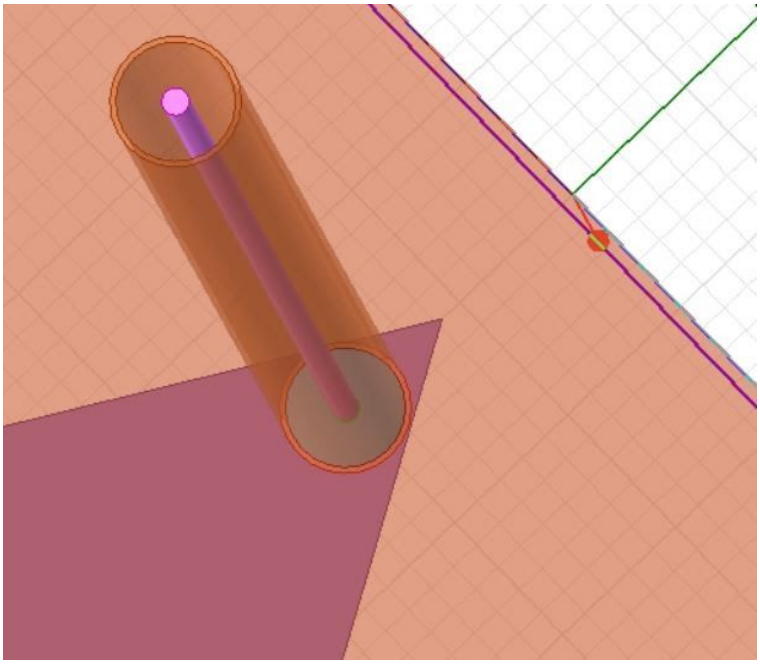

Figure 1C. Coaxial feed close up attached in ground plane.

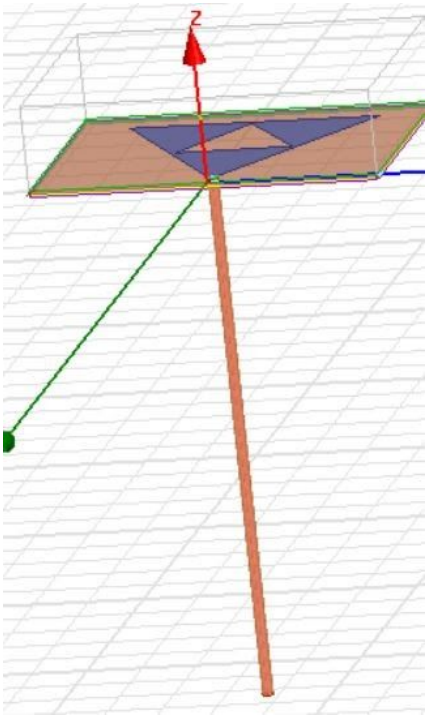

Figure 2C. Far view of cable and patch antenna.